Bandwidths limitations of giant optical field enhancements in dielectric multi-layers

Myriam Zerrad, Aude L. Lereu, Cesaire N'diaye, Fabien Lemarchand, Claude Amra

Research Article | Vol. 25, No. 13 | 26 Jun 2017 | OPTICS EXPRESS 14883
Optics EXPRESS

Bandwidths limitations of giant optical field enhancements in dielectric multi-layers

M. ZERRAD,[1,3] A. L. LEREU,[1,4] C. N'DIAYE,[2] F. LEMARCHAND,[1] AND C. AMRA[1,5]

[1] *Aix Marseille Univ, CNRS, Centrale Marseille, Institut Fresnel, Marseille, France*
[2] *Ecole Supérieure Polytechnique, Université Cheikh Anta Diop - Dakar, Senegal*
[3] *myriam.zerrad@fresnel.fr*
[4] *aude.lereu@fresnel.fr*
[5] *claude.amra@fresnel.fr*

Abstract: Dielectric multilayers, when properly optimized, have been shown to sustain giant optical field enhancement directly linked to the imaginary index of the materials. Such giant optical field is of great interests to increase tremendously the sensitivity of optoelectronic systems. Unfortunately, this ultra-sensitive system is also highly depending on the illumination conditions. We discuss here the effect of the angular divergence and the spectral bandwidth of the incident laser beam on the absorption and field enhancement. In this study, we clearly show that giant optical field enhancements, up to several decades, may be achievable when the incident conditions are down few μrad and pm in term of angular and spectral bandwidths respectively.

OCIS codes: (240.0310) Thin films; (240.6690) Surface waves, (220.4610) Optical fabrication

References and links

1. P. Yeh, A. Yariv, and A. Y. Cho, "Optical surface waves in periodic layered media," Appl. Phys. Lett. **32**(2), 104–106 (1978).
2. W. Ng, P. Yeh, P. C. Chen and A. Yariv, "Optical surface waves in periodic layered medium grown by liquid phase epitaxy," Appl. Phys. Lett. **32**(6), 370–372 (1978).
3. P. Yeh, A. Yariv and C-S. Hong, "Electromagnetic propagation in periodic stratified media. I. General theory," J. Opt. Soc. Am. **67**(4), 423–438 (1977).
4. A. Yariv and P. Yeh, "Electromagnetic propagation in periodic stratified media. II. Birefringence, phase matching, and x-ray lasers," J. Opt. Soc. Am. **67**(4), 438–447 (1977).
5. N. Ashby and S. C. Miller, "Interference theory of reflection from multilayered media," J. Opt. Soc. Am. **67**(4), 448–453 (1977).
6. E. R. Mendieta and P. Halevi, "Electromagnetic surface modes of a dielectric superlattice: the supercell method," J. Opt. Soc. Am. B **14**(2), 370–381 (1997).
7. W. M. Robertson and M. S. May, "Surface electromagnetic wave excitation on one-dimensional photonic band-gap arrays," Appl. Phys. Lett. **74**(13), 1800–1802 (1999).
8. K. Mehrany, S. Khorasani and B. Rashidian, "Novel optical devices based on surface wave excitation at conducting interfaces," Semicond. Sci. Technol. **18**, 582–588 (2003).
9. J. Martorell, D. W. L. Sprung and G. V. Morozov, "Surface TE waves on 1D photonic crystals," J. Opt. A: Pure Appl. Opt. **8**, 630–638 (2006).
10. F. Michelotti, A. Sinibaldi, P. Munzert, N. Danz, and E. Descrovi, "Probing losses of dielectric multilayers by means of Bloch surface waves," Opt. Lett. **38**(5), 616–618 (2013).
11. L. Gao, F. Lemarchand, and M. Lequime, "Exploitation of multiple incidences spectrometric measurements for thin film reverse engineering," Opt. Express **20**(14), 15734–15751 (2012).
12. R. C. Nesnidal and T. G. Walker, "Multilayer dielectric structure for enhancement of evanescent waves," Appl. Opt. **35**(13), 2226–2229 (1996).
13. R. Sainidou, J. Renger, T. V. Teperik, M-U. Gonzalez, R. Quidant, and F. J. Garcia de Abajo, "Extraordinary All-Dielectric Light Enhancement over Large Volumes," Nano Lett. **10**(11), 4450–4455 (2010).
14. C. Ndiaye, F. Lemarchand, M. Zerrad, D. Ausserré, and C. Amra, "Optimal design for 100% absorption and maximum field enhancement in thin-film multilayers at resonances under total reflection," Appl. Opt. **50**(9), C382–C387 (2011).
15. C. Amra, C. Ndiaye, M. Zerrad and F. Lemarchand, "Optimal design for field enhancement in optical coatings," Proc. SPIE **8168**, 8168–8174, (2011).

#291801 https://doi.org/10.1364/OE.25.014883
Journal © 2017 Received 31 Mar 2017; revised 1 Jun 2017; accepted 3 Jun 2017; published 20 Jun 2017

Optics EXPRESS

16. A. L. Lereu, M. Zerrad, C. Ndiaye, F. Lemarchand and C. Amra, "Scattering losses in multidielectric structures designed for giant optical field enhancement," Appl. Opt. **53**(4), A412–A416 (2014).
17. A. Yariv, "Universal relations for coupling of optical power between microresonators and dielectric waveguides," Electron. Lett. **36**(4), 321–322 (2000).
18. M. Tsang and D. Psaltis, "Reflectionless evanescent wave amplification via two dielectric planar waveguides," Opt. Lett. **31**(18), 2741–2743 (2006).
19. R. Kaiser, Y. Lévy, N. Vansteenkiste, A. Aspect, W. Seifert, D. Leipold and J. Mlynek, "Resonant enhancement of evanescent waves with a thin dielectric waveguide," Opt. Comm. **104**(4–6), 234–240 (1994).
20. G. Labeyrie, A. Landragin, J. Von Zanthier, R. Kaiser, N. Vansteenkiste, C. Westbrook and A. Aspect, "Detailed study of a high-finesse planar waveguide for evanescent wave atomic mirrors," Quantum Semiclass. Opt. **8**, 603–627 (1996).
21. P. C. Ke, X. S. Gan, J. Szajman, S. Schilders, and M. Gu, "Optimizing the strength of an evanescent wave generated from a prism coated with a double-layer thin-film stack," Bioimaging **5**(1), 1–8 (1997).
22. M. D. Perry, R. D. Boyd, J. A. Britten, D. Decker, B. W. Shore, C. Shannon and E. Shults, "High-efficiency multilayer dielectric diffraction gratings," Opt. Lett. **20**(8), 940–942 (1995).
23. Jeun Kee Chua, V. M. Murukeshan, "Resonant amplification of frustrated evanescent waves by single dielectric coating," Opt. Commun. **283**(1), 169–175 (2010).
24. E. Descrovi, T. Sfez, L. Dominici,W. Nakagawa, F. Michelotti, F. Giorgis and H-P. Herzig, "Near-field imaging of Bloch surface waves on silicon nitride one-dimensional photonic crystals," Opt. Express **16**(8), 5453–5464 (2008).
25. C. Ndiaye, M. Zerrad, A. L. Lereu, R. Roche, Ph. Dumas, F. Lemarchand and C. Amra, "Giant optical field enhancement in multi-dielectric stacks by photon scanning tunneling microscopy," Appl. Phys. Lett. **103**, 131102 (2013).
26. A. L. Lereu, M. Zerrad, M. Petit, F. de Fornel and C. Amra, "Multi-dielectric stacks as a platform for giant optical field," Proc. SPIE **9162**, 916219 (2014).
27. A. Shalabney and I. Abdulhalim, "Electromagnetic fields distribution in multilayer thin film structures and the origin of sensitivity enhancement in surface plasmon resonance sensors," Sens. Actuat. A **159**(1), 24–32 (2010).
28. A. Sinibaldi, N. Danz, E. Descrovic, P. Munzert, U. Schulz, F. Sonntag, L. Dominici, F. Michelotti, "Direct comparison of the performance of Bloch surface wave and surface plasmon polariton sensors," Sens. Actuat. B **174**, 292–298 (2012).
29. Wan YuHang, Zheng Zheng, Shi XiaoGang, Bian YuSheng and Liu JianSheng, "Hybrid plasmon waveguide leveraging Bloch surface polaritons for sub-wavelength confinement,"" Sci. China Tech. Sci. **56**(3), 567–572 (2013).
30. R. Badugu, E. Descrovi, J. R. Lakowic, "Radiative Decay Engineering 7: Tamm State-Coupled Emission Using a Hybrid Plasmonic-Photonic Structure," Anal.l Biochem. **445**, 1–13 (2014).
31. Z. Sekkat, S. Hayashi, D. V. Nesterenko, A. Rahmouni, S. Refki, H. Ishitobi, Y. Inouye and S. Kawata, "Plasmonic coupled modes in metal-dielectric multilayer structures: Fano resonance and giant field enhancement," Opt. Exp. **24**(18), 20080–20088 (2016).
32. W. A. Challener, J. D. Edwards, R. W. McGowan, J. Skorjanec and Z. Yang, "A multilayer grating-based evanescent wave sensing technique," Sens. Actuat. B **71**(1–2), 42–46 (2000).
33. M. Ballarini, F. Frascella, F. Michelotti, G. Digregorio, P. Rivolo, V. Paeder, V. Musi, F. Giorgis and E. Descrovi, "Bloch surface waves-controlled emission of organic dyes grafted on a one dimensional photonic crystal," Appl. Phys. Lett. **99**, 043302 (2011).
34. M. Ballarini, F. Frascella, E. Enrico, P. Mandracci, N. De Leo, F. Michelotti, F. Giorgis and E. Descrovi, "Bloch surface waves-controlled fluorescence emission: coupling into nanometer-sized polymeric waveguides," Appl. Phys. Lett. **100**, 063305 (2012).
35. S. Pirotta, X. G. Xu, A. Delfan, S. Mysore, S. Maiti, G. Dacarro, M. Patrini, M. Galli, G. Guizzetti, D. Bajoni, J. E. Sipe, G. C. Walker and M. Liscidini, "Surface-Enhanced Raman Scattering in Purely Dielectric Structures via Bloch Surface Waves," J. Phys. Chem. C **117**(13), 6821–6825 (2013).
36. K. Toma, E. Descrovi, M. Toma, M. Ballarini, P. Mandracci, F. Giorgis, A. Mateescu, U. Jonas, W. Knoll and J. Dostalek, "Bloch surface wave-enhanced fluorescence biosensor," Biosens. Bioelectron. **43**, 108–114 (2013).
37. F. Frascella, S. Ricciardi, P. Rivolo, V. Moi, F. Giorgis, E. Descrovi, F. Michelotti, P. Munzert, N. Danz, L. Napione, M. Alvaro and F. Bussolino, "A Fluorescent One-Dimensional Photonic Crystal for Label-Free Biosensing Based on Bloch Surface Waves," Sensors **13**(2), 2011–2022 (2013).
38. M. Lequime and C. Amra, *De l'Optique Electromagnétique à l'Interférométrie*, (EDP Sciences, 2013).

1. Introduction

Dielectric multi-layers have been widely investigated using either Bloch waves and band structures considerations [1–10] or optical thin film concept [11–16]. In both cases, very sharp resonances, spectrally and angularly, are anticipated. In addition, dielectrics are low losses materials, i.e. low imaginary part of the refractive index, and therefore they are usually used for optical guiding [17, 18]. The resulting modes induced large evanescent waves at the

Optics EXPRESS

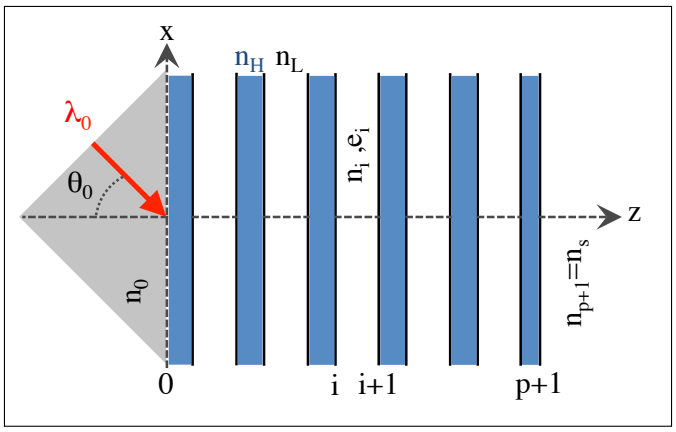

Fig. 1. Typical dielectric multi-layer and the used analytical parameters. For all the numerical work presented here we have used n_0=1.52, n_H=2.141, n_L=1.46, n_S=1 for a TE-polarized incident beam at 633 nm with an incidence at 45°. Note that the choice of n_H and n_L were done in reference to the refractive indices of Ta_2O_5 and SiO_2 respectively. Different optimizations are then carried out for $10^{-2}<n"_p<10^{-5}$.

interfaces that lend dielectric multi-layers even more interests. Kaiser *et al* [19–21] reported an enhancement factor of 1000 using m-line measurements, while Perry *et al* [22] demonstrated an improvement of the 1^{st} order of diffraction by a grating-based multi-dielectric stack. Jeun Kee Chua *et al* [23] numerically optimized a four layers stack to achieve a full transmission. Finally, optical near field measurements have also been done by Descrovi *et al* [24] evidencing an enhancement factor of 100 over a dielectric multi-layer. And more recently we measured an enhancement factor of 300 for an optimized dielectric multi-layer [25, 26].

By supporting large field enhancements, dielectric multi-layers are also envisioned for sensing applications, where they are typically compared with surface plasmon resonances as related in [27–29], or combined with plasmon effect as Tamm plasmon [30] or in Fano resonance with giant field enhancement [31]. Challener *et al* [32] reported large field enhancements together with a penetration depth larger than surface plasmons. Ballarini *et al* [33, 34] demonstrated fluorescent emission enhanced by the resulting Bloch surface waves in a dielectric multi-layer. More recently, bio-sensing applications-based dielectric multi-layers have also been reported [35–37] showing their growing interest. However, drawbacks are inevitable, in the literature, attenuation sources, i.e. both the incident conditions and the multi-layer depositions, are always mentioned to achieve this giant field enhancement. However, to the best of our knowledge the attenuation sources have not been quantified.

In this paper, we quantify the resonance attenuations, resulting from the illumination conditions, by looking at the absorption and field enhancement. We report on analytical and numerical work evaluating the relevance of controlling incident conditions. We will consider dielectric multi-layers (DM) of different imaginary parts of the index of refraction. We will tackle the effect of the incident beam angular divergence followed by the incident spectral bandwidth over the resonance. We will then concluded in Section 4. Note that errors in the fabrication of the DM are not considered here but are the second source of attenuations. We therefore assumed here no fabrication variations by considering a dedicated resonant DM at θ_R and λ_R.

Optics EXPRESS

2. Analytical results

Designing dielectric multi-layer was carried out using the admittance formalism under total internal reflection (T = 0), by optimizing the absorption to be total (A = 100%, R = 0) and therefore obtaining a giant field enhancement (proportional to the inverse imaginary index), see details on the optimization method in [14, 15]. Fig. 1 gives the used parameters to described an optimized DM with an imaginary index n_p'' in the top layer, and with the resonance angle θ_R and wavelength λ_R. We recently reported on the experimental and numerical variations of the reflectance of such DM while varying the incident angle (θ) around θ_R and extracted the field enhancement for various incident angles using near field scanning optical microscopy [16, 25, 26]. Let's now focus on the effects of the illumination conditions over the resonance, starting with the spatial divergence and followed by the spectral bandwidth.

2.1. Effect of the illumination divergence

We first suppose that the incident wavelength $\lambda_0 = \lambda_R$, meaning we neglect the spectral variations of the illumination. An incident beam usually spread angularly around the average illumination incidence θ_0. This spatial divergence of the beam, noted $\Delta\theta_0$, will be considered in the spatial frequencies domain.

The electromagnetic field of a progressive and monochromatic beam in free space is described in the most general case by a spatial waves packet written, at any point (x, z) of the space, as follow:

$$E_0(x,z) = \int_\sigma A_0^+(\sigma - \sigma_0)\exp[j(\sigma x + \alpha z)]\,\mathrm{d}\sigma \tag{1}$$

where the average spatial pulsation σ_0 is expressed as:

$$\sigma_0 = k_0 \sin\theta_0 = \frac{2\pi}{\lambda_0} n_0 \sin\theta_0 \tag{2}$$

and σ, representing all the pulsations included in the wave packet, is given by:

$$\sigma = \frac{2\pi}{\lambda_0} n_0 \sin\theta \qquad \forall\,\theta \in \left[\theta_0 - \frac{\Delta\theta_0}{2}, \theta_0 + \frac{\Delta\theta_0}{2}\right]. \tag{3}$$

In addition, we are in the propagative regime, i.e. without evanescent waves, and in a transparent incident medium, meaning that:

$$\sigma < k \quad \Rightarrow \quad \alpha = \sqrt{k_0^2 - \sigma^2} \quad \in \mathbb{R}. \tag{4}$$

Equation (3) shows that the energy is essentially distributed over the spatial divergence $\Delta\theta_0$. We will use thereafter a gaussian beam to model the energy decay around the average pulsation. The reflected field for the resonant DM can now be deduced from equation (1), by weighting each frequency contribution of the incident field by the corresponding amplitude reflection coefficient $r(\sigma)$. This gives from equation (1):

$$E_r(x,z) = \int_\sigma A_0^+(\sigma - \sigma_0) r(\sigma) \exp[j(\sigma x - \alpha z)]\,\mathrm{d}\sigma. \tag{5}$$

Such relationship has been largely used to study the spatial shape of the reflected beam at resonance conditions, which is mainly driven by the presence of complex poles in the amplitude reflection factor. We notice here that the local field depends on the phase properties of the reflection. Now, as far as the global energy is concerned, one can use another relationship

Optics EXPRESS

which does not depend on this phase distribution. Indeed one can show [38] that the flow of the Poynting vectors related to the fields, describing the incident (equation (1)) and reflected (equation (5)) beams, are respectively proportional to:

$$\phi_0^+ = \int_\sigma \alpha(\sigma)|A_0^+(\sigma-\sigma_0)|^2\,\mathrm{d}\sigma, \tag{6}$$

$$\phi_0^- = \int_\sigma \alpha(\sigma)R(\sigma)|A_0^+(\sigma-\sigma_0)|^2\,\mathrm{d}\sigma, \tag{7}$$

with $R(\sigma) = |r(\sigma)|^2$ the reflection coefficient in intensity for each spatial frequency. In total reflection, meaning with no transmission, the absorption of the DM lighten by the waves packet is written as $A = 1 - R$, that is, using equations (6) and (7):

$$A(\theta_0, \Delta\theta_0) = 1 - \frac{\phi_0^-}{\phi_0^+} = \frac{1}{\phi_0^+}\int_\sigma \alpha(\sigma)[1-R(\sigma)]|A_0^+(\sigma-\sigma_0)|^2\,\mathrm{d}\sigma. \tag{8}$$

This shows that the absorption depends on the average illumination incidence θ_0 and beam divergence $\Delta\theta_0$ which are characteristic of the illumination. The average illumination incidence is indeed described by the average pulsation σ_0, while the divergence is included in the function $A(\sigma)$. However, one has to keep in mind that the results will also depend on the DM, namely its resonance angle θ_R and its imaginary index n_R''. Therefore, the result can be seen as the product of the incident energy distribution $A^2(\sigma)$, centered at σ_0 with a width $\Delta\sigma$, with the reflection function R(σ) centered at σ_R with a width $\Delta\sigma_R$. R(σ) is linked to the DM resonance properties, while A(σ) characterize the illumination.

For a first approximation, the incident beam is taken here to be 1D gaussian with a width L at $1/e$, and the electric field associated with the incident light is written, in a plane perpendicular to the propagation, as such:

$$E^2(x') = E_0^2 e^{-(\frac{x'}{L})^2}, \tag{9}$$

and the flow of the incident Poynting vectors is thus written as:

$$\phi_0^+ = \sqrt{\pi}LE_0^2. \tag{10}$$

In addition, due to Parseval theorem, the amplitude distribution $A^2(\sigma)$ can be written as:

$$A_0^{+2}(\sigma) = E_0^2\,TF_{1D}\left\{e^{-(\frac{x'}{L})^2}\right\} = E_0^2\,\frac{L}{2\pi}exp\left[-\left(\frac{L\sigma}{2\pi}\right)^2\right]. \tag{11}$$

The quantity L describing the Gaussian beam at $1/e$ is therefore linked to the beam divergence $\Delta\theta_0$ by:

$$\frac{L\sigma_{max}}{2\pi} = 1, \Rightarrow \quad \sigma_{max} = \frac{2\pi}{L} = \frac{2\pi}{\lambda_0}n_o\sin\Delta\theta_0 \approx \frac{2\pi}{\lambda_0}n_0\Delta\theta_0, \Leftrightarrow \quad \Delta\theta_0 \approx \frac{\lambda_0}{n_0 L}. \tag{12}$$

In general, a laser divergence is in the order of 1 mrad, we can therefore make the approximation that $\sin(\Delta\theta_0) \approx \Delta\theta_0$ to connect the beam divergence $\Delta\theta_0$ to the size L of the laser spot. At this stage, we are able to quantify numerically the influence of divergence on the absorption decay on the field enhancement (see Section 3).

2.2. Effect of the illumination spectral bandwidth

Performances of the optimized DM can also be improved by controlling the spectral bandwidth $\Delta\omega$ of the illumination. We neglect here the angular divergence effect, showed in the previous subsection, in order to separate the variables. Therefore we assume here that the illumination

Optics EXPRESS

incidence is the same as the DM resonance angle ($\theta_0 = \theta_R$). Similarly to section 2.1, we can assume here a frequency waves packet with a spectral width $\Delta\lambda_0$ around the emission wavelength λ_0. The resonance wavelength is taken to be λ_R. The incident waves packet, in the Fourier space can therefore be decomposed as a continuous sum of plane waves of different temporal pulsations. The flow of the incident and reflected Poynting vectors can be expressed as equations (5) and (6) respectively, by solving the integral over the temporal pulsation ω instead of the spatial pulsation σ.

From there, we can express (as in equation (8)) the absorption for the temporal waves packet as:

$$A(\lambda_0, \Delta\lambda_0) = 1 - \frac{\phi_0^-}{\phi_0^+} = \frac{1}{\phi_0^+} \int_\omega \alpha(\omega)[1 - R(\omega)]|A_0^+(\omega - \omega_0)|^2 \, \mathrm{d}\omega. \tag{13}$$

Knowing that $\omega = \frac{2\pi c}{\lambda}$, with c the speed of light, one can link the frequency interval $\Delta\omega$ to the one of wavelength $\Delta\lambda$ by:

$$\Delta\omega = \frac{2\pi c}{\lambda^2}\Delta\lambda \tag{14}$$

Equation (13) can then be expressed as such:

$$A(\lambda_0, \Delta\lambda_0) = 1 - \frac{\phi_0^-}{\phi_0^+} = \frac{2\pi c}{\phi_0^+} \int_\lambda \alpha(\lambda)[1 - R(\lambda)]|A_0^+(\lambda - \lambda_0)|^2 \frac{\mathrm{d}\lambda}{\lambda^2}. \tag{15}$$

Depending on the light source, the spectral bandwidth can vary up to tens of nm. We will numerically evidence the $\Delta\lambda$ effect of the illumination on the DM resonance by looking at the influence on the absorption expressed in equation (15) and the associated field enhancement.

3. Numerical results and effect of the illumination bandwidths on the resonance

3.1. From the absorption point of view

In the previous section, we presented the analytical method evaluating the resonances in term of absorption when taking into account the illumination angular or spectral apertures. We now numerically estimate, in Fig. 2(a), the divergence effect on the resonance absorption of a dielectric multi-layer, designed for $n"_p = 10^{-3}$ and illuminated with a perfect plane wave (black line) or with waves packets presenting angular apertures of $\Delta\theta = 0.1$ mrad (red line) and $\Delta\theta = 1$ mrad (blue line). We clearly show a decrease of the absorption by about 20% and 80% with respect to the perfect plane wave for both considered cases. Similarly, we show, in Fig. 2(b), the spectral bandwidth effect for an illumination beam with no spectral dispersion (black line) and with spectral bandwidths of $\Delta\lambda = 0.1$ nm (red line) and 1 nm (blue line). The absorption undergoes an attenuation by about 10% and 40% for the two spectral bandwidths we considered. Note that when considering an excitation with an angular divergence we do not introduce spectral dispersion and vice versa.

The angular divergence has a stronger effect on the absorption attenuation than the spectral bandwidth. In addition, it is relatively easy to work with a spectral bandwidth of 0.1 nm whereas controlling a beam divergence down to less than 0.1 mrad is more complicate. This first results show the relative importance of controlling excitation beam parameters to access to the predicted strong and sharp resonances. We then perform a numerical study on the absorption for a panel of DMs with different imaginary part of the refractive index (n''_p) for the top layer. We report, in Fig. 3, the maximum of absorption for each n''_p case as a function of the angular (a) or spectral (b) illumination bandwidths, defined respectively by equations (8) and (15).

As expected, as the n''_p decreases, the resonance becomes sharper which requires to adjust the control of the illumination bandwidths accordingly. In order to link to the experimental limitations, the grey hatched parts on Fig. 3 mark the up-to-date achievable experimental conditions. We clearly show that for any proposed optimized DMs, a spectral control down to

Optics EXPRESS

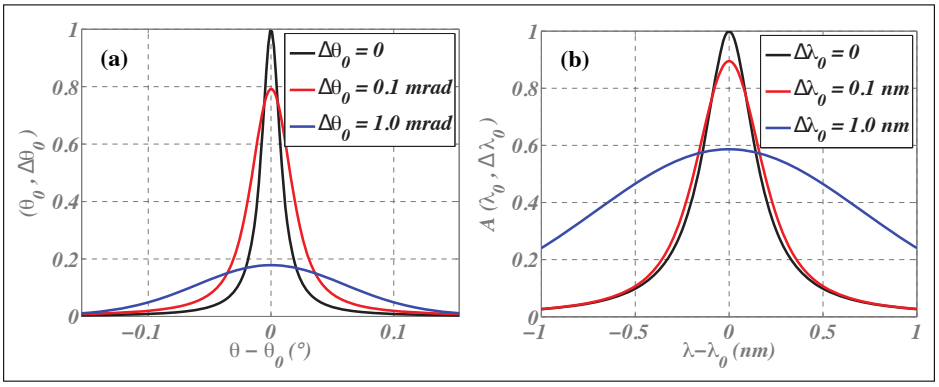

Fig. 2. Numerical evidences of the angular divergence ($\Delta\theta$) (a) and the spectral bandwidth ($\Delta\lambda$) (b) of the illumination for a dielectric multi-layer with an absorptive top layer of imaginary index $n_p'' = 10^{-3}$. The absorption is optimized to be 100% when $\Delta\theta$ and $\Delta\lambda$ equal 0. In (a) we add angular divergences of $\Delta\theta$=0.1 mrd (red line) and 1 mrd divergence (blue line) that induce a drop in the absorption by ≈ 80% and 20%, respectively. In (b), for spectral bandwidths of $\Delta\lambda$ =0.1 nm (red line) or 1 nm (blue line), the absorption falls to 90% and 60% respectively.

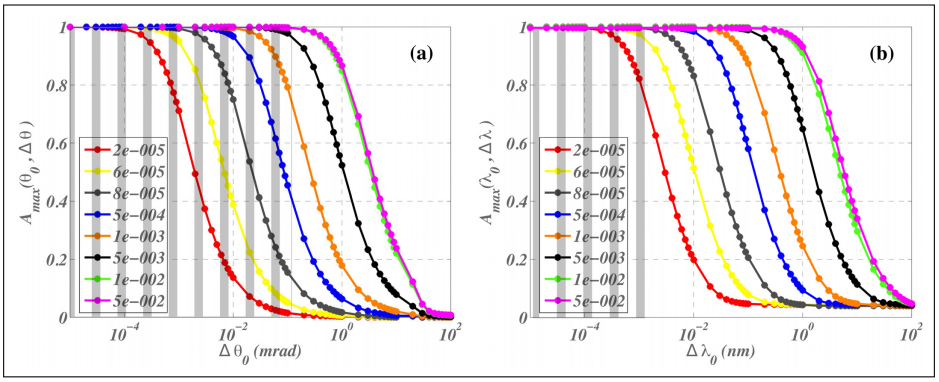

Fig. 3. Numerical calculations of the measurable absorption as a function of illumination angular divergence $\Delta\theta$ (a) or as a function of the spectral bandwidth $\Delta\lambda$ (b). Optimized DMs with absorptive top layers of imaginary indices n_p'' from 2.10^{-5} up to 5.10^{-2} are considered. The hatched regions mark the experimental limitations that cannot be achievable currently.

Table 1. **Summary of the angular and spectral divergences effect over the absorption for four optimized DMs of different n_p''.**

n_p"	10^{-2}	10^{-3}	10^{-4}	10^{-5}	10^{-2}	10^{-3}	10^{-4}	10^{-5}
% Absorption	Angular divergence $\Delta\theta$ (mrad)				Spectral divergence $\Delta\lambda$ (nm)			
100 %	0.35	0.002	6.10^{-5}	$6.6.10^{-5}$	0.2	8.10^{-3}	6.10^{-5}	6.10^{-5}
80 %	3	0.097	0.028	$7.3.10^{-4}$	3.2	0.15	10^{-3}	10^{-3}
20 %	28	0.88	0.25	$6.8.10^{-3}$	30	1.4	10^{-2}	10^{-2}

Optics EXPRESS

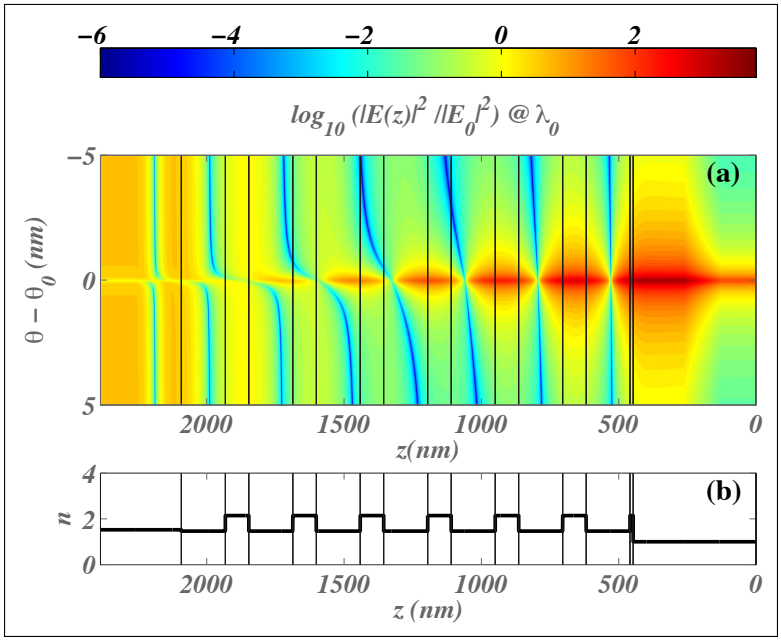

Fig. 4. (a) Representation in logarithmic scale of the spectral evolution of the electromagnetic field within an optimized dielectric multi-layer designed for $n"_p = 10^{-3}$ when illuminated by the left side through a silica prism. Black lines represent interfaces of the dielectric multi-layer, and the right side of the DM is the field in Air, i.e. the emergent medium. (b) gives the evolution of optical indexes of each layer within the structure.

the picometer is sufficient to get at least 80% of absorption. Contrariwise, the angular dispersion is commonly experimentally controlled down to 0.1 mrad only. Under this condition, we get 80% of absorption for DMs optimized with a n''_p ranging from 10^{-3} to 10^{-2} (see Fig. 3). For DMs with $n''_p > 10^{-4}$, the experimental absorption is below 60% with a 0.1 mrad divergence. To clearly quantify the bandwidths, we summarized some performances in term of absorption in Table 1 as a function a angular divergence and spectral divergence. This investigation gives "realistic" limitations of such optical resonances, sustained in dielectric multi-layer, in term of absorption. We show that by taking into account the spectral or angular bandwidths of illumination in the calculation, we can predict, for a given component, both the experimentally reachable absorption at resonance associated to the resulting field enhancement. In other words, we propose here a method allowing predictions of resonant dielectric multi-layers performances under realistic conditions of use. Next, we will investigate the illumination bandwidths issues in term of field enhancement. We will highlight a broadening of the resonance escorting the absorption amplitude losses as the bandwidths get larger.

3.2. *From the field enhancement point of view*

Resonances based on total absorption lead to electromagnetic (EM) field enhancements with a factor proportional to $1/n"_p$, where $n"_p$ is the imaginary index of the last layer [14, 15]. Since the reflection, absorption and field enhancement are somehow linked, if the illumination bandwidths affect the absorption, they will certainly affect the resulting EM field enhancement. To illustrate this point, for the same structure studied in the subsection 3.1), we display, in Fig. 4, the spatial evolution of the calculated EM field within the DM as a function of the illumination spectral aperture. We used a logarithmic scale in order to magnify the contraste and highlight

Optics EXPRESS

the effect onto the EM field enhancement. A similar mapping was obtained when considering the illumination angular divergence (data not shown).

On this mapping, the zero line represents the resonance case where no bandwidths effects are introduced. We clearly see the large field enhancement at the interface with the emergent medium. As we increase the illumination spectral bandwidth (up to ± 5 nm), we observe modifications of the field distribution throughout the DM and a frank decrease of the field enhancement factor at the last interface down to few dozens. In addition, the penetration depth within the emergent medium is also reduced as the bandwidths increase. Fig. 4 confirms our conclusion given in section 3.1), that the control and/or estimations of the illumination bandwidths play a key role in the fundamental and applied investigations of such multi-dielectric resonances on both absorption and field enhancement aspects.

4. Conclusion

In conclusion, we have investigated analytically and numerically, the effect of the angular divergence and spectral bandwidth of the illumination source over sharp resonances supported by dielectric multi-layers. The absorption and field enhancement were studied for DMs optimized with different imaginary indices for the absorptive top layer. We demonstrated that the angular divergence is the most critical parameter to control. For example, an angular divergence controlled at 0.1 mrad is required to achieve a full field enhancement of 10^3 (i.e. for a DM with an absorptive top layer of imaginary index $n''_p = 10^{-3}$). For the spectral bandwidth, the effect is not as critical as one can experimentally control it down to the picometer, which already allows to access to field enhancements up to few 10^5. We also show that, as the field enhancement factor increases, the illumination bandwidths effects are more pronounced. We demonstrated the critical influence of the illumination conditions in order to obtain giant field enhancements and compared with the current experimental conditions achievable. We show that field enhancement up few 10^3 can be achieved when controlling $\Delta\theta$ at 2 μrad and $\Delta\lambda$ at 10 pm. Note, nevertheless, that 20% of an expected field enhancement of 10^4-10^5 may still be of great interest in specific applications.

Achieving ultra-sensitive resonances is doable using dielectric multi-layer but the intrinsic limitations reside in the required experimental conditions to actually get the giant field enhancements. Indeed, the characteristic of a highly sensitive system is to drastically react with its environment. This is of great interest for sensing applications to detect very low concentrations and volumes but required specific attention in adjusting the external illumination conditions as well as fabrication parameters and errors that we did not mention here. This study paves the way toward “realistic" uses of giant fields sustained in multi-dielectrics.

Acknowledgments

The authors acknowledge the CNRS; the Aix-Marseille Université; the Ecole Centrale Marseille; and the région PACA for financial support. This work was initiated during the project “SEEC-Surface enhanced ellipsometric contrast" funded by the ANR-Agence Nationale de la Recherche.